On-Off-Based Secure Transmission Design with Outdated Channel State Information

Jianwei Hu, *Student Member, IEEE,* Weiwei Yang, *Member, IEEE,* Nan Yang, *Member, IEEE,*
Xiangyun Zhou, *Member, IEEE,* and Yueming Cai, *Senior Member, IEEE*

***Abstract*—We design new secure on-off transmission schemes in wiretap channels with outdated channel state information (CSI). In our design we consider not only the outdated CSI from the legitimate receiver but two distinct scenarios, depending on whether or not the outdated CSI from the eavesdropper is known at the transmitter. Under this consideration our schemes exploit the useful knowledge contained in the available outdated CSI, based on which the transmitter decides whether to transmit or not. We derive new closed-form expressions for the transmission probability, the connection outage probability, the secrecy outage probability, and the reliable and secure transmission probability to characterize the achievable performance. Based on these results, we present the optimal solutions that maximize the secrecy throughput under dual connection and secrecy outage constraints. Our analytical and numerical results offer detailed insights into the design of the wiretap coding parameters and the imposed outage constraints. We further show that allowing more freedom on the codeword transmission rate enables a larger feasible region of the dual outage constraints by exploiting the trade-off between reliability and security.**

***Index Terms*—Secure transmission, on-off scheme, outdated CSI, outage constraints, secrecy throughput.**

I. Introduction

THE INHERENT openness of the wireless medium makes wireless data transmission difficult to be shielded from unintended recipients. As such, secure transmission over wireless channels becomes a critical issue in the design of wireless networks. Traditionally, security is viewed as an independent feature guaranteed through higher layer techniques, e.g., cryptographic protocols, assuming that an error-free physical layer link has already been established [1]. In large scale dynamic wireless networks, however, the high complexity of key distribution and management makes it difficult to achieve the required security level with cryptographic methods alone [2]. In contrast to cryptographic protocols, physical layer security exploits the statistics of the channel at the physical layer to protect wireless transmission against eavesdropping [3], [4]. Therefore, it has been widely recognized as a complement to cryptographic protocols for security enhancement and thus attracted enormous research efforts recently.

A. Background

The information-theoretical foundation of physical layer security was laid down by Shannon's definition of perfect secrecy in [5]. Based on [5], [6] introduced the wiretap channel model as a basic framework for physical layer security. The results in [6] were subsequently generalized to the broadcast channel and the Gaussian channel in [7] and [8], respectively. These early studies revealed that if the eavesdropper's observation is a degraded version of the legitimate user's observation, it is possible to provide information-theoretically secure communication between the legitimate users while keeping the eavesdropper completely ignorant of secure messages.

A key assumption underpinning the information-theoretical contributions in [6]–[8] is that perfect channel state information (CSI) from both the legitimate receiver and the eavesdropper is available at the transmitter. However, this assumption may not be realistic since the uncertainty in CSI is a common factor that affects the performance of practical communication systems. In particular, if the eavesdropper is a passive user, knowing the CSI from the eavesdropper is almost impossible. Moreover, the perfect knowledge of the legitimate user's channel may not be easy to obtain at the transmitter in practice, due to the limitations incurred by signal processing techniques such as channel estimation errors, finite-rate feedback links, and outdated CSI (or delayed CSI).

Against this background, a growing body of research efforts have recently been devoted to examining the impact of imperfect CSI on physical layer security. Considering the practical passive eavesdropping scenario, [9]–[13] proposed transmit antenna selection schemes to enhance security in wiretap channels. Considering Gaussian-distributed errors produced by imperfect channel estimation at the legitimate receiver, [14]–[19] designed secure transmission schemes and investigated the achievable performance. It is worth mentioning that [19] successfully introduced on-off design to develop fixed-rate and variable-rate secure transmission schemes in the presence of channel estimation errors. Considering limited feedback constraints, [20]–[24] characterized the secrecy performance in multi-antenna systems and studied the optimal power allocation applied in artificial-noise-aided beamforming. Note

This work of J. Hu, W. Yang and Y. Cai was supported by the National Natural Science Foundation of China (No. 61371122, No. 61471393 and No. 61501512) and Jiangsu provincial National Science Foundation (BK20150718). The work of N. Yang and X. Zhou was supported by the Australian Research Council Discovery Project (DP150103905).

J. Hu, W. Yang, and Y. Cai are with the College of Communications Engineering, PLA University of Science and Technology, Nanjing 210007, China (e-mail: hujianwei1990@yeah.net, wwyang1981@163.com, caiym@vip.sina.com).

N. Yang and X. Zhou are with the Research School of Engineering, Australian National University, Canberra, ACT 0200, Australia (email: {nan.yang, xiangyun.zhou}@anu.edu.au).

Digital Object Identifier 10.1109/TVT.2015.2477427

that [24] also adopted on-off design to develop the optimized artificial-noise-aided transmission scheme in limited feedback channels. Although [9]–[24] have developed signal processing techniques with passive eavesdropping, imperfect channel estimation and limited feedback constraints, the models and methods used in these papers cannot be used to address another practical environment where imperfect CSI is caused by the time delay of feedback link. This motivates us to develop new models and methods for physical layer security with outdated CSI.

B. Motivation

Outdated CSI is a practical contributor to the uncertainty of channel knowledge at communication nodes. In a practical system with feedback delay from the receiver to the transmitter, the CSI obtained at the transmitter may be an outdated version of the actual CSI. As such, the obtained CSI cannot be directly used for secure transmission. Along this line there are limited studies in the literature [25], [26]. Specifically, [25] derived an upper bound on the secrecy rate loss by exploiting the Gauss-Markov fading spectrum to model the feedback delay, while [26] analyzed the effects of outdated CSI on the secrecy outage performance of multi-input single-output wiretap channels with transmit antenna selection. Notably, [25], [26] merely concentrated on the secrecy performance analysis, but have not presented detailed transmission design in the presence of outdated CSI.

It is well to be reminded that although the outdated CSI is not equivalent to the actual CSI, the temporal correlation between outdated CSI and actual CSI makes it possible for the transmitter to exploit some knowledge offered by the outdated CSI to perform secure transmission. Therefore, there arises a significant problem to be addressed: *"how can we take advantage of this benefit to design secure transmission schemes?"* Recall that the on-off design, as an efficient approach that guarantees transmission quality, has been successfully used to develop transmission schemes in the presence of channel estimation errors [19] and limited feedback constraints [24], respectively. Motivated by this, in this work we adopt the on-off design to develop secure transmission schemes in the presence of outdated CSI.

C. Contributions

We develop new secure transmission schemes in the presence of outdated CSI by using on-off design to exploit the useful information existed in the outdated CSI. These schemes are designed for two distinct scenarios, depending on whether or not the eavesdropper is a legitimate user served by the transmitter. In *Scenario 1*, the eavesdropper is an active user (but not the intended receiver) and the outdated CSI from both the legitimate receiver and the eavesdropper is available at the transmitter. In *Scenario 2*, the eavesdropper is not a legitimate user and only the outdated CSI from the legitimate receiver is available at the transmitter. The on-off design adopted in our developed schemes allows transmission only when the channel qualities known at the transmitter satisfy some predetermined requirements [19], [24], [27], [28]. The rationale behind the on-off design is that transmission should be avoided when the quality of the intended receiver's channel is poor or the quality of the eavesdropper's channel is strong.

Our primary contributions are summarized as follows:

- We design new on-off transmission schemes in the presence of outdated CSI and then derive new closed-form expressions for the connection outage probability, the secrecy outage probability, and the reliable and secure transmission probability to quantify the achievable performance. Different from [19], [24], [28], for the first time we incorporate the reliable and secure transmission probability into the formulation of the throughput, forming the *secrecy throughput*. Notably, the secrecy throughput measures the average rate of the message which is successfully decoded at the legitimate receiver while being kept confidential to the eavesdropper.
- We determine new rate selection strategies that exploit the useful information existed in the outdated CSI. In these strategies, the codeword transmission rate is adaptively designed according to the feedback from the legitimate receiver. The secrecy rate is optimally selected to maximize the secrecy throughput subject to the constraints on the connection outage probability and secrecy outage probability. We present the optimal design for both Scenario 1 and *Scenario 2*.
- We reach an important conclusion that allowing more freedom on the codeword transmission rate enables the enhancement of the reliability level by exploiting the trade-off between reliability and security, since the codeword transmission rate without optimization leads to the poor reliability performance. We further show that this trade-off provides us with a profound extension in the feasible region of reliability constraint.

D. Organization

The remainder of this paper is organized as follows. Section II details the outdated CSI model, the on-off transmission schemes and the wiretap codes design in wiretap channels. In Section III, we derive the exact expressions for the performance metrics and offer numerical results to investigate the secrecy performance. In Section IV, the optimized secrecy rates for each scenario are presented, and the illustrative numerical results are provided. Some discussions and concluding remarks are provided in Sections V and VI, respectively.

II. Secure Transmission in the Presence of Outdated CSI

We consider a wiretap channel where the message transmitted from a source Alice to a destination Bob is intercepted by an eavesdropper Eve. We assume that Alice, Bob, and Eve are equipped with a single antenna each. Throughout this paper, we refer to the Alice-Bob channel as the main channel and refer to the Alice-Eve channel as the eavesdropper's channel. We assume that both channels are subject to Rayleigh fading. We also assume independent but non-identical distributions between the main channel and the eavesdropper's channel such that they have different average signal-to-noise ratios (SNRs).

Prior to data transmission, Alice requests Bob to feed back his instantaneous channel quality by sending pilot signals. Aided by the pilot signals, Bob estimates the main channel coefficient, h_b, and calculates the instantaneous received SNR as $\gamma_b = P_b|h_b|^2/\sigma_b^2$, where P_b and σ_b^2 denote the average received signal power at Bob and the additive white Gaussian noise (AWGN) power at Bob, respectively; while Eve estimates the eavesdropper's channel coefficient, h_e, and calculates the instantaneous received SNR as $\gamma_e = P_e|h_e|^2/\sigma_e^2$, where P_e and σ_e^2 denote the average received signal power at Eve and the AWGN power at Eve, respectively. Then Bob feeds back γ_b to Alice to facilitate wiretap codes design. Whether or not Eve feeds back γ_e depends on whether or not Eve is an active user of the network. Specifically, we consider two scenarios based on the availability of γ_e in this work, as follows:

- *Scenario 1*: Eve is a non-passive eavesdropper such that γ_e is fed back to Alice. This scenario represents the case where Eve is an active user of the network but is treated as a malicious eavesdropper when Alice performs secure transmission to Bob [29]–[31].
- *Scenario 2*: Eve is a passive eavesdropper such that γ_e is not fed back to Alice. This scenario represents the case where Eve is an illegitimate user of the network [9]–[13].

We clarify that in both scenarios Eve is a regular user served by Alice and thus Eve's distance from Alice is known and the path loss exponent is known. That is, Alice always knows the average received SNR at Eve, $\bar{\gamma}_e$. Based on the feedback information, Alice calculates the instantaneous channel capacity of the main channel during pilot transmission as $C_b = \log_2(1+\gamma_b)$. Moreover, in *Scenario 1* Alice calculates the instantaneous channel capacity of the eavesdropper's channel capacity as $C_e = \log_2(1+\gamma_e)$; while in *Scenario 2* Alice calculates the average channel capacity of the eavesdropper's channel capacity as $\bar{C}_e = \log_2(1+\bar{\gamma}_e)$. Then Alice adaptively designs the wiretap codes based on C_b and C_e in *Scenario 1* but based on C_b and $\bar{C}_e$ in *Scenario 2*.

A. Outdated CSI

In this work, we concentrate on the practical wiretap channel where the CSI obtained at Alice is outdated. In the practice, the process of acquiring CSI at the transmitter may take a significant time duration for pilot transmission, channel estimation, and CSI feedback. This results in the fact that the channel coefficients during data transmission are not h_b and h_e. As such, the CSI obtained at Alice is an imprecise version of the actual CSI, which causes the uncertainty in channel quality.

We first describe the uncertainty in the channel knowledge obtained at Alice in the wiretap channel. We define $\tilde{h}_b$ and $\tilde{h}_e$ as the τ_d time-delayed versions of h_b and h_e, respectively. Using a Gauss-Markov process [32], we formulate $\tilde{h}_b$ and $\tilde{h}_e$ as

$$\tilde{h}_b = \rho_b h_b + \sqrt{1-\rho_b^2}\, w_b \qquad (1)$$

and

$$\tilde{h}_e = \rho_e h_e + \sqrt{1-\rho_e^2}\, w_e, \qquad (2)$$

respectively, where $w_b \sim \mathcal{CN}(0,1)$ and $w_e \sim \mathcal{CN}(0,1)$ are the channel-independent errors in the main channel and the eavesdropper's channel, respectively. Here, ρ_b denotes the correlation coefficient between $\tilde{h}_b$ and h_b, while ρ_e denotes the correlation coefficient between $\tilde{h}_e$ and h_e. In the Clark's fading model, ρ_b and ρ_e can be expressed as $\rho_b = J_0(2\pi f_b \tau_d)$ and $\rho_e = J_0(2\pi f_e \tau_d)$, where $J_0(\cdot)$ is the zeroth-order Bessel function of the first kind, f_b and f_e are the maximum Doppler frequencies at Bob and Eve, respectively. In the Gaussian fading model, ρ_b and ρ_e can be expressed as $\rho_b = \exp(-\pi^2 f_b^2 \tau_d^2)$ and $\rho_e = \exp(-\pi^2 f_e^2 \tau_d^2)$, from which we find that ρ_b and ρ_e degrade monotonically to zero as τ_d increases. Since the Jakes model is widely adopted in the existing studies on mobile radios [32], in this work we use this model to perform the simulations in Section III-C, Section IV-C and Section V. Therefore, the received signals at Bob and Eve during data transmission are given by

$$y_b = \tilde{h}_b\sqrt{P_b}x + n_b = \left(\rho_b h_b + \sqrt{1-\rho_b^2}\, w_b\right)\sqrt{P_b}x + n_b \qquad (3)$$

and

$$y_e = \tilde{h}_e\sqrt{P_e}x + n_e = \left(\rho_e h_e + \sqrt{1-\rho_e^2}\, w_e\right)\sqrt{P_e}x + n_e, \qquad (4)$$

respectively, where $n_b \sim \mathcal{CN}\left(0,\sigma_b^2\right)$ and $n_e \sim \mathcal{CN}\left(0,\sigma_e^2\right)$ denote the AWGN at Bob and Eve, respectively. Based on (3) and (4), the instantaneous SNRs at Bob and Eve during data transmission are given by $\tilde{\gamma}_b = |\tilde{h}_b|^2 P_b/\sigma_b^2$ and $\tilde{\gamma}_e = |\tilde{h}_e|^2 P_e/\sigma_e^2$, respectively. Of course, $\tilde{\gamma}_b$ and $\tilde{\gamma}_e$ cannot be obtained at Alice.

B. On-Off Schemes and Performance Metrics

We adopt Wyner's encoding strategy [6] for secure transmission in the presence of outdated CSI. Before each transmission block, Alice needs to choose two rate parameters for wiretap codes design, i.e., the codeword transmission rate, R_b, and the secrecy rate, R_s. The rate redundancy, $R_b - R_s$, provides secrecy against eavesdropping. We clarify that R_b and R_s hold constant over the duration of a block. In this work we use on-off schemes for *Scenario 1* and *Scenario 2*, as done in [19], [28], which are detailed as follows:

- On-off scheme for *Scenario 1*: Based on the feedback from Bob and Eve, Alice obtains the channel capacity of the main channel, C_b, and the channel capacity of the eavesdropper's channel C_e. As such, Alice uses C_b and C_e to design wiretap codes and performs data transmission only when $C_b - C_e > R_s$.
- On-off scheme for *Scenario 2*: Based on the feedback from Bob, Alice only obtains C_b. By aid of the statistic knowledge of the eavesdropper's channel, Alice uses C_b and $\bar{C}_e$ to design wiretap codes and performs data transmission only when $C_b - \bar{C}_e > R_s$.

It is worthwhile to note that perfect connection and perfect secrecy between Alice and Bob cannot be guaranteed in the presence of outdated CSI for both cases. This is due to the uncertainty in channel knowledge, i.e., Alice has no knowledge of the actual main channel capacity given by $\tilde{C}_b = \log_2(1+\tilde{\gamma}_b)$ and the actual eavesdropper's channel capacity given by $\tilde{C}_e = \log_2(1+\tilde{\gamma}_e)$. As such, the connection outage occurs when $\tilde{C}_b < R_b$, in which Bob is unable to decode the received codewords correctly. Mathematically, the connection outage probability, p_{co}, is defined as [19, Eq. (16)]

$$p_{co} = \Pr\left\{\tilde{C}_b < R_b \,|\text{transmission}\right\}. \qquad (5)$$

Moreover, the secrecy outage occurs when $R_b - R_s < \tilde{C}_e$. Mathematically, the secrecy outage probability, p_{so}, is defined as [19, Eq. (15)]

$$p_{so} = \Pr\left\{R_b - R_s < \tilde{C}_e \,|\text{transmission}\right\}. \qquad (6)$$

Note that both outage probabilities are conditioned upon a message being transmitted. These outage probabilities are of practical importance since the reliability level and the security level can be measured using these probabilities when the outdated CSI is in presence. However, from (5) and (6) we find that the connection outage event and the secrecy outage event are definitely not independent from each other, but related with R_b. To evaluate the combination of reliability and security, we resort to the successful (reliable and secure) transmission probability, p_{rst}, which is defined as

$$p_{rst} = \Pr\left\{\tilde{C}_b \geq R_b, R_b - R_s \geq \tilde{C}_e \,|\text{transmission}\right\}. \qquad (7)$$

Notably, (7) is a novel formulation to characterize the reliability and security levels of transmission.

C. Rate Selection Strategy

To exploit the useful knowledge existing in the outdated CSI, the strategy for the choice of R_b and R_s is explained as following: R_b is adaptively designed according to the feedback from the legitimate receiver, while R_s is optimally chosen and keeps constant over the transmission block. In other words, this is an adaptive-codeword-transmission-rate but fixed-secrecy-rate strategy. Since C_b is the only knowledge obtained from Bob, it is convenient and natural for Alice to set $R_b = C_b$ to guarantee maximum rate redundancy against eavesdropping. This leads to the fact that R_s is the only controllable parameter in the wiretap codes design. As such, R_s is optimally chosen before data transmission and then kept constant during data transmission.

The aim of our design is to achieve the optimal secrecy throughput under the constraints of two outage probabilities. Here, the secrecy throughput, η, is defined as

$$\eta = p_{tx} p_{rst} R_s, \qquad (8)$$

where p_{tx} denotes the transmission probability and p_{rst} is given by (7). *We highlight that the secrecy throughput in* (8) *is different from the throughput in [19], defined as* $p_{tx}(1-p_{co})R_s$. In (8), we introduce p_{rst} into the formulation of the secrecy throughput. We clarify that the incorporation of p_{rst} is reasonable and necessary for the assessment and improvement of reliability and security. Specifically, p_{rst} jointly quantizes the reliability level and the security level of the secrecy throughput.

Using (8), our design aim is formulated as

$$\begin{aligned} &\max_{R_s} \quad \eta, \\ &\text{subject to} \quad p_{co} \leq \epsilon, p_{so} \leq \delta, \end{aligned} \qquad (9)$$

where ϵ denotes the reliability constraint and δ denotes the security constraint. Note that solving the optimized R_s in (9) can help us not only obtain good secrecy throughput performance but keep the reliability and security levels under control.

III. Secrecy Performance with On-off Transmission Schemes

In this section, we analyze the secrecy performance for the two scenarios presented in Section II-B by exploiting the on-off transmission schemes. Specifically, we derive the closed-form expressions for the connection outage probability, the secrecy outage probability as well as the reliable and secure transmission probability defined in Section II-B. We then present the numerical results to examine the performance of the on-off transmission schemes with outdated CSI.

A. Performance Analysis for Scenario 1

In this subsection, we consider *Scenario 1* and derive new expressions for the connection outage probability, the secrecy outage probability, the reliable and secure transmission probability. We then present the feasibility of the reliability constraint and the security constraint as well.

1) $p_{tx_1}(R_s)$, $p_{co_1}(R_s)$, $p_{so_1}(R_s)$ *and* $p_{rst_1}(R_s)$*:* In *Scenario 1*, Alice sets $R_b = C_b$ and performs data transmission only when $C_b - C_e \geq R_s$. The transmission probability in *Scenario 1* is derived as

$$\begin{aligned} p_{tx_1}(R_s) &= \Pr\left\{C_b - C_e \geq R_s\right\} \\ &= \Pr\left\{\gamma_b \geq 2^{R_s}(1+\gamma_e) - 1\right\} \\ &= \int_0^\infty f_{\gamma_e}(\gamma_e)\left(\int_{2^{R_s}(1+\gamma_e)-1}^\infty f_{\gamma_b}(\gamma_b)\, d\gamma_b\right) d\gamma_e \\ &= \frac{\bar{\gamma}_b}{\bar{\gamma}_b + 2^{R_s}\bar{\gamma}_e}\exp\left(-\frac{2^{R_s}-1}{\bar{\gamma}_b}\right). \end{aligned} \qquad (10)$$

We note that (10) can be obtained by using the probability density functions (PDFs) of γ_b and γ_e. In this work, we assume that both the main channel and the eavesdropper's channel are subject to Rayleigh fading, such that the PDF of γ_b is $f_{\gamma_b}(\gamma_b) = \exp(-\gamma_b/\bar{\gamma}_b)/\bar{\gamma}_b$ and the PDF of γ_e is $f_{\gamma_e}(\gamma_e) = \exp(-\gamma_e/\bar{\gamma}_e)/\bar{\gamma}_e$ [19], where $\bar{\gamma}_b = \mathbb{E}\left[h_b^2\right]P_b/\sigma_b^2$ denotes the average SNR at Bob and $\bar{\gamma}_e = \mathbb{E}\left[h_e^2\right]P_e/\sigma_e^2$ denotes the average SNR at Eve.

The connection outage occurs when $\tilde{C}_b < C_b$. As such, the connection outage probability in *Scenario 1* is given by

$$p_{co_1}(R_s) = \Pr\left\{\tilde{C}_b < C_b \,|C_b - C_e \geq R_s\right\}. \qquad (11)$$

Based on the cumulative density distribution (CDF) of a non-central chi-square distributed variable, we derive $p_{co_1}(R_s)$ as

$$\begin{aligned} p_{co_1}(R_s) =& 1-\frac{\bar{\gamma}_b+2^{R_s}\bar{\gamma}_e}{\bar{\gamma}_b}\exp\left(-\frac{\left(1+\rho_b^2\right)\left(2^{R_s}-1\right)}{\left(1-\rho_b^2\right)\bar{\gamma}_b}\right) \\ &\times\sum_{n=0}^{\infty}\sum_{k=0}^{\infty}\frac{\rho_b^{2(n+k)}\left(1-\rho_b^2\right)\Gamma(n+2k+1)}{k!2^{n+2k+1}\Gamma(n+k+1)} \\ &\times\sum_{m=0}^{n+2k}\sum_{q=0}^{m}\frac{\left(2^{R_s}-1\right)^{m-q}2^{m+qR_s}}{(m-q)!(\left(1-\rho_b^2\right)\bar{\gamma}_b)^m\bar{\gamma}_e} \\ &\times\left(\frac{\left(1-\rho_b^2\right)\bar{\gamma}_b\bar{\gamma}_e}{\left(1-\rho_b^2\right)\bar{\gamma}_b+2^{R_s+1}\bar{\gamma}_e}\right)^{q+1}, \end{aligned} \quad (12)$$

where $\Gamma(\cdot)$ is the Gamma function defined in [33, Eq. (8.310.1)]. The proof is given in Appendix A.

The secrecy outage occurs when $C_b-R_s<\tilde{C}_e$. As such, the secrecy outage probability in *Scenario 1* is given by

$$p_{so_1}(R_s)=\Pr\left\{C_b-R_s<\tilde{C}_e\left|C_b-C_e\geq R_s\right.\right\}. \quad (13)$$

We derive $p_{so_1}(R_s)$ as

$$p_{so_1}(R_s)=\frac{\bar{\gamma}_b+2^{R_s}\bar{\gamma}_e}{\bar{\gamma}_b}\exp\left(\frac{2^{R_s}-1}{\bar{\gamma}_b}\right)(\ell_1-\ell_2), \quad (14)$$

where ℓ_1 is

$$\begin{aligned} \ell_1 =& \exp\left(-\frac{2^{-R_s}-1}{\left(1-\rho_e^2\right)\bar{\gamma}_e}\right)\sum_{n=0}^{\infty}\sum_{k=0}^{\infty}\frac{\rho_e^{2(n+k)}\left(1-\rho_e^2\right)}{\Gamma(k+1)(\left(1-\rho_e^2\right)\bar{\gamma}_e)^k} \\ &\times\sum_{q=0}^{k}\binom{k}{q}\frac{\left(1-2^{R_s}\right)^{k-q}}{2^{kR_s}\bar{\gamma}_b}\left(\frac{\left(1-\rho_e^2\right)2^{R_s}\bar{\gamma}_b\bar{\gamma}_e}{\bar{\gamma}_b+\left(1-\rho_e^2\right)2^{R_s}\bar{\gamma}_e}\right)^{q+1} \\ &\times\Gamma\left(q+1,\frac{\bar{\gamma}_b+\left(1-\rho_e^2\right)2^{R_s}\bar{\gamma}_e}{\left(1-\rho_e^2\right)2^{R_s}\bar{\gamma}_b\bar{\gamma}_e}\left(2^{R_s}-1\right)\right), \end{aligned} \quad (15)$$

ℓ_2 is

$$\begin{aligned} \ell_2 =& \exp\left(-\frac{2^{1-R_s}-2}{\left(1-\rho_e^2\right)\bar{\gamma}_e}\right)\sum_{n=0}^{\infty}\sum_{k=0}^{\infty}\frac{\rho_e^{2(n+k)}\left(1-\rho_e^2\right)}{k!(\left(1-\rho_e^2\right)\bar{\gamma}_e)^k} \\ &\times\sum_{m=0}^{n+k}\sum_{q=0}^{k+m}\binom{k+m}{q}\frac{\left(2^{-R_s}-1\right)^{k+m-q}2^{-qR_s}}{m!(\left(1-\rho_e^2\right)\bar{\gamma}_e)^m\bar{\gamma}_b} \\ &\times\Gamma\left(q+1,\frac{2^{1-R_s}\bar{\gamma}_b+\left(1-\rho_e^2\right)\bar{\gamma}_e}{\left(1-\rho_e^2\right)\bar{\gamma}_b\bar{\gamma}_e}\left(2^{R_s}-1\right)\right) \\ &\times\left(\frac{\left(1-\rho_e^2\right)\bar{\gamma}_b\bar{\gamma}_e}{2^{1-R_s}\bar{\gamma}_b+\left(1-\rho_e^2\right)\bar{\gamma}_e}\right)^{q+1}, \end{aligned} \quad (16)$$

and $\Gamma(\cdot,\cdot)$ is the incomplete Gamma function defined in [33, Eq. (8.352.2)]. The proof is given in Appendix B.

The successful transmission occurs when both $\tilde{C}_b\geq C_b$ and $C_b-R_s\geq\tilde{C}_e$ are satisfied simultaneously. As such, the reliable and secure transmission probability in *Scenario 1* is given by

$$p_{rst_1}(R_s)=\Pr\left\{\tilde{C}_b\geq C_b, C_b-R_s\geq\tilde{C}_e\left|C_b-C_e\geq R_s\right.\right\}. \quad (17)$$

We derive $p_{rst_1}(R_s)$ as

$$p_{rst_1}(R_s)=\frac{\bar{\gamma}_b+2^{R_s}\bar{\gamma}_e}{\bar{\gamma}_b}\exp\left(\frac{2^{R_s}-1}{\bar{\gamma}_b}\right)(\ell_3-\ell_4-\ell_5), \quad (18)$$

where ℓ_3 is

$$\begin{aligned} \ell_3 =& \sum_{n=0}^{\infty}\sum_{k=0}^{\infty}\frac{\rho_b^{2(n+k)}\left(1-\rho_b^2\right)}{\Gamma(k+1)\Gamma(n+k+1)2^{n+2k+1}} \\ &\times\Gamma\left(n+2k+1,\frac{2\left(2^{R_s}-1\right)}{\left(1-\rho_b^2\right)\bar{\gamma}_b}\right), \end{aligned} \quad (19)$$

ℓ_4 is

$$\begin{aligned} \ell_4 =& \exp\left(-\frac{2^{-R_s}-1}{\bar{\gamma}_e}\right)\sum_{n=0}^{\infty}\sum_{k=0}^{\infty}\frac{\rho_b^{2(n+k)}\left(1-\rho_b^2\right)}{\Gamma(k+1)\Gamma(n+k+1)} \\ &\times\Gamma\left(n+2k+1,\frac{\left(2^{R_s+1}\bar{\gamma}_e+\left(1-\rho_b^2\right)\bar{\gamma}_b\right)}{\left(2^{R_s}-1\right)^{-1}\left(1-\rho_b^2\right)2^{R_s}\bar{\gamma}_b\bar{\gamma}_e}\right) \\ &\times\left(\frac{2^{R_s}\bar{\gamma}_e}{2^{R_s+1}\bar{\gamma}_e+\left(1-\rho_b^2\right)\bar{\gamma}_b}\right)^{n+2k+1}, \end{aligned} \quad (20)$$

and $\ell_5=\ell_6-\ell_7$, where ℓ_6 and ℓ_7 are given at the top of next page. The proof is given in Appendix C.

Remark 1: We clarify that the connection outage probability is merely affected by ρ_b, as indicated by (12), and the secrecy outage probability is merely affected by ρ_e, as indicated by (14). This reveals that in *Scenario 1*, the reliability level depends on the outdated CSI of the main channel, while the security level depends on the outdated CSI of the eavesdropper's channel.

2) Feasibility of Constraints: We now investigate the feasibility of the reliability constraint and the security constraint. Using the mathematical software package to take the first derivative of $p_{co_1}(R_s)$ in (12), we find that $p_{co_1}(R_s)$ is an increasing function of R_s. When $R_s\to 0$, $p_{co_1}(R_s)$ achieves its lower bound, $p_{co_1,LB}$. We obtain $p_{co_1,LB}$ as

$$\begin{aligned} p_{co_1,LB} =& 1-\sum_{n=0}^{\infty}\sum_{k=0}^{\infty}\frac{\rho_b^{2(n+k)}\Gamma(n+2k+1)}{\Gamma(k+1)\Gamma(n+k+1)2^{n+2k+1}} \\ &\times\sum_{m=0}^{n+2k}\frac{\left(1-\rho_b^2\right)^2(\bar{\gamma}_b+\bar{\gamma}_e)2^m\bar{\gamma}_e^m}{\left(2\bar{\gamma}_e+\left(1-\rho_b^2\right)\bar{\gamma}_b\right)^{m+1}}. \end{aligned} \quad (23)$$

As such, the feasible range of the reliability constraint in *Scenario 1* is given by

$$p_{co_1,LB}<\epsilon\leq 1. \quad (24)$$

We then take the first derivative of $p_{so_1}(R_s)$ in (14) and find that $p_{so_1}(R_s)$ is also an increasing function of R_s. When $R_s\to 0$, $p_{so_1}(R_s)$ achieves its lower bound, $p_{so_1,LB}$. We obtain $p_{so_1,LB}$ as

$$\begin{aligned} p_{so_1,LB} =& \frac{\bar{\gamma}_b+\bar{\gamma}_e}{\bar{\gamma}_b}\sum_{n=0}^{\infty}\sum_{k=0}^{\infty}\left(\frac{\rho_e^{2(n+k)}\left(1-\rho_e^2\right)^2\bar{\gamma}_e\bar{\gamma}_b^k}{\left(\bar{\gamma}_b+\left(1-\rho_e^2\right)\bar{\gamma}_e\right)^{k+1}}\right. \\ &\left.-\sum_{m=0}^{n+k}\binom{m+k}{m}\frac{\rho_e^{2(n+k)}\left(1-\rho_e^2\right)^2\bar{\gamma}_e\bar{\gamma}_b^{m+k}}{\left(2\bar{\gamma}_b+\left(1-\rho_e^2\right)\bar{\gamma}_e\right)^{m+k+1}}\right). \end{aligned} \quad (25)$$

$$\begin{aligned}\ell_6 =&\exp\left(-\frac{2^{-R_s}-1}{\left(1-\rho_e^2\right)\bar{\gamma}_e}\right)\sum_{n=0}^{\infty}\sum_{k=0}^{\infty}\sum_{s=0}^{\infty}\sum_{t=0}^{\infty}\frac{\rho_b^{2(n+k)}\rho_e^{2(s+t)}\left(1-\rho_b^2\right)\left(1-\rho_e^2\right)\left(\left(1-\rho_e^2\right)\bar{\gamma}_e\right)^{n+2k-t+1}}{k!\Gamma\left(n+k+1\right)t!\left(2\left(1-\rho_e^2\right)\bar{\gamma}_e+2^{-R_s}\left(1-\rho_b^2\right)\bar{\gamma}_b\right)^{n+2k+1}}\sum_{q=0}^{t}\frac{t!\left(2^{-R_s}-1\right)^{t-q}}{q!\left(t-q\right)!}\\&\times\left(\frac{2^{-R_s}\left(1-\rho_b^2\right)\left(1-\rho_e^2\right)\bar{\gamma}_b\bar{\gamma}_e}{2\left(1-\rho_e^2\right)\bar{\gamma}_e+2^{-R_s}\left(1-\rho_b^2\right)\bar{\gamma}_b}\right)^q\Gamma\left(n{+}2k{+}q{+}1,\frac{2\left(1-\rho_e^2\right)\bar{\gamma}_e+2^{-R_s}\left(1-\rho_b^2\right)\bar{\gamma}_b}{\left(2^{R_s}-1\right)^{-1}\left(1-\rho_b^2\right)\left(1-\rho_e^2\right)\bar{\gamma}_b\bar{\gamma}_e}\right),\end{aligned}\tag{21}$$

$$\begin{aligned}\ell_7 =&\exp\left(-\frac{2^{1-R_s}-2}{\left(1-\rho_e^2\right)\bar{\gamma}_e}\right)\sum_{n=0}^{\infty}\sum_{k=0}^{\infty}\sum_{s=0}^{\infty}\sum_{t=0}^{\infty}\frac{\rho_b^{2(n+k)}\rho_e^{2(s+t)}\left(1-\rho_b^2\right)\left(1-\rho_e^2\right)}{\left(2\left(1-\rho_e^2\right)\bar{\gamma}_e+2^{1-R_s}\left(1-\rho_b^2\right)\bar{\gamma}_b\right)^{n+2k+1}}\sum_{m=0}^{s+t}\sum_{q=0}^{t+m}\frac{\left(\left(1-\rho_e^2\right)\bar{\gamma}_e\right)^{n+2k-t-m+1}}{\Gamma\left(n+k+1\right)\left(t+m-q\right)!}\\&\times\frac{\left(2^{-R_s}-1\right)^{t+m-q}}{\left(\left(t+m\right)!\right)^{-1}k!t!m!q!}\left(\frac{2^{-R_s}\left(1-\rho_b^2\right)\left(1-\rho_e^2\right)\bar{\gamma}_b\bar{\gamma}_e}{2\left(1-\rho_e^2\right)\bar{\gamma}_e+2^{1-R_s}\left(1-\rho_b^2\right)\bar{\gamma}_b}\right)^q\Gamma\left(n{+}2k{+}q{+}1,\frac{2\left(1-\rho_e^2\right)\bar{\gamma}_e+2^{1-R_s}\left(1-\rho_b^2\right)\bar{\gamma}_b}{\left(2^{R_s}-1\right)^{-1}\left(1-\rho_b^2\right)\left(1-\rho_e^2\right)\bar{\gamma}_b\bar{\gamma}_e}\right).\end{aligned}\tag{22}$$

Accordingly, we obtain the feasible range of the security constraint in *Scenario 1* as

$$p_{so_1,LB}<\delta\leq 1.\tag{26}$$

We highlight that in *Scenario 1* the reliability constraint and the security constraint are feasible only when (24) and (26) are satisfied.

B. Performance Analysis for Scenario 2

In this subsection, we concentrate on *Scenario 2*. New closed-form expressions are derived for the transmission probability, connection outage probability, secrecy outage probability, reliable and secure transmission probability, based on which we evaluate the feasibility of the reliability and security constraints.

1) $p_{tx_2}\left(R_s\right)$, $p_{co_2}\left(R_s\right)$, $p_{so_2}\left(R_s\right)$, and $p_{rst_2}\left(R_s\right)$: In *Scenario 2*, Alice has no knowledge of C_e. As such, Alice sets $R_b=C_b$ and performs secure transmission only when $C_b-\bar{C}_e\geq R_s$. The transmission probability in *Scenario 2* is derived as

$$\begin{aligned}p_{tx_2}\left(R_s\right)&=\Pr\left\{C_b-\bar{C}_e\geq R_s\right\}\\&=\Pr\left\{\gamma_b\geq 2^{R_s}\left(1+\bar{\gamma}_e\right)-1\right\}\\&=\int_{2^{R_s}\left(1+\bar{\gamma}_e\right)-1}^{\infty}f_{\gamma_b}\left(\gamma_b\right)d\gamma_b\\&=\exp\left(-\frac{2^{R_s}\left(1+\bar{\gamma}_e\right)-1}{\bar{\gamma}_b}\right).\end{aligned}\tag{27}$$

The connection outage probability in *Scenario 2* is given by

$$p_{co_2}\left(R_s\right)=\Pr\left\{\tilde{C}_b<C_b\left|C_b-\bar{C}_e\geq R_s\right.\right\}.\tag{28}$$

Applying the CDF of a non-central chi-square distributed variable, $p_{co_2}\left(R_s\right)$ is derived as

$$\begin{aligned}p_{co_2}\left(R_s\right)=&1-\exp\left(\frac{2^{R_s}\left(1+\bar{\gamma}_e\right)-1}{\bar{\gamma}_b}\right)\sum_{n=0}^{\infty}\sum_{k=0}^{\infty}\frac{1}{\Gamma\left(k+1\right)}\\&\times\Gamma\left(n+2k+1,\frac{2^{R_s+1}\left(1+\bar{\gamma}_e\right)-2}{\left(1-\rho_b^2\right)\bar{\gamma}_b}\right)\\&\times\left(\frac{1}{2}\right)^{n+2k+1}\frac{\rho_b^{2(n+k)}\left(1-\rho_b^2\right)}{\Gamma\left(n+k+1\right)}.\end{aligned}\tag{29}$$

The secrecy outage probability in *Scenario 2* is given by

$$p_{so_2}\left(R_s\right)=\Pr\left\{C_b-R_s<\tilde{C}_e\left|C_b-\bar{C}_e\geq R_s\right.\right\}.\tag{30}$$

Using the statistics of γ_b and $\tilde{\gamma}_e$, we derive $p_{so_2}\left(R_s\right)$ as

$$p_{so_2}\left(R_s\right)=\frac{2^{R_s}\bar{\gamma}_e\exp\left(-1\right)}{2^{R_s}\bar{\gamma}_e+\bar{\gamma}_b}.\tag{31}$$

The reliable and secure transmission probability in *Scenario 2* is given by

$$p_{rst_2}\left(R_s\right)=\Pr\left\{\tilde{C}_b\geq C_b,C_b{-}R_s\geq\tilde{C}_e\left|C_b-\bar{C}_e\geq R_s\right.\right\}.\tag{32}$$

We derive $p_{rst_2}\left(R_s\right)$ as

$$p_{rst_2}\left(R_s\right)=\exp\left(\frac{2^{R_s}\left(1+\bar{\gamma}_e\right)-1}{\bar{\gamma}_b}\right)\left(\ell_8-\ell_9\right),\tag{33}$$

where ℓ_8 is

$$\begin{aligned}\ell_8 =&\sum_{n=0}^{\infty}\sum_{k=0}^{\infty}\frac{\rho_b^{2(n+k)}\left(1-\rho_b^2\right)}{\Gamma\left(k+1\right)\Gamma\left(n+k+1\right)}\left(\frac{1}{2}\right)^{n+2k+1}\\&\times\Gamma\left(n+2k+1,\frac{2\left(2^{R_s+1}\left(1+\bar{\gamma}_e\right)-2\right)}{\left(1-\rho_b^2\right)\bar{\gamma}_b}\right),\end{aligned}\tag{34}$$

and ℓ_9 is

$$\begin{aligned}\ell_9 =&\exp\left(-\frac{2^{-R_s}-1}{\bar{\gamma}_e}\right)\sum_{n=0}^{\infty}\sum_{k=0}^{\infty}\frac{\rho_b^{2(n+k)}\left(1-\rho_b^2\right)}{\Gamma\left(k+1\right)\Gamma\left(n+k+1\right)}\\&\times\Gamma\left(n{+}2k{+}1,\frac{\left(2^{R_s+1}\bar{\gamma}_e{+}\left(1{-}\rho_b^2\right)\bar{\gamma}_b\right)\left(\bar{\gamma}_b\bar{\gamma}_e\right)^{-1}}{\left(2^{R_s}\left(1+\bar{\gamma}_e\right)-1\right)^{-1}2^{R_s}\left(1{-}\rho_b^2\right)}\right)\\&\times\left(\frac{2^{R_s}\bar{\gamma}_e}{2^{R_s+1}\bar{\gamma}_e+\left(1-\rho_b^2\right)\bar{\gamma}_b}\right)^{n+2k+1}.\end{aligned}\tag{35}$$

Remark 2: Based on (29) and (31), we find that the connection outage probability is only affected by ρ_b but the secrecy outage probability is not influenced by either ρ_b or ρ_e. This reveals that in *Scenario 2* the outdated CSI only influences the reliability level.

2) Feasibility of Constraints: We next examine the feasibility of the reliability constraint and the security constraint. Using the mathematical software package to take the first-order derivative of $p_{co_2}(R_s)$ in (29), we find that $p_{co_2}(R_s)$ is an increasing function of R_s. When $R_s \to 0$, $p_{co_2}(R_s)$ achieves its lower bound, $p_{co_2,LB}$, which is derived as

$$p_{co_2,LB} = 1 - \exp\left(\frac{\bar{\gamma}_e}{\bar{\gamma}_b}\right) \sum_{n=0}^{\infty} \sum_{k=0}^{\infty} \frac{\rho^{2(n+k)}\left(1-\rho^2\right)}{\Gamma(k+1)\Gamma(n+k+1)} \times \left(\frac{1}{2}\right)^{n+2k+1} \Gamma\left(n+2k+1, \frac{2\bar{\gamma}_e}{\left(1-\rho^2\right)\bar{\gamma}_b}\right). \tag{36}$$

Therefore, the feasible range of the reliability constraint in *Scenario 2* is given by

$$p_{co_2,LB} < \epsilon \leq 1. \tag{37}$$

Next, by observing (31) we see that $p_{so_2}(R_s)$ is also an increasing function of R_s. When $R_s \to 0$, $p_{so_2}(R_s)$ achieves its lower bound, $p_{so_2,LB}$, given by

$$p_{so_2,LB} = \frac{\bar{\gamma}_e \exp(-1)}{\bar{\gamma}_e + \bar{\gamma}_b}. \tag{38}$$

Thus, the feasible range of the security constraint in *Scenario 2* is obtained as

$$p_{so_2,LB} < \delta \leq 1. \tag{39}$$

It is worthwhile to note that in *Scenario 2* the reliability constraint and the security constraint are feasible only when (37) and (39) are satisfied.

C. Numerical Results

We present numerical results in this subsection to examine the performance of the on-off transmission schemes. We clarify that the infinitive summations in our derived closed-form expressions can be perfectly approximated with finite summations (usually first 10 terms in the summations give an accurate approximation). The simulation settings are as follows, unless specified otherwise: The average received SNR at Bob is assumed to be $P_b/\sigma_b^2 = 10$ dB, while the average received SNR at Eve is assumed to be $P_e/\sigma_e^2 = 0$ dB. In each simulation trial, the main channel coefficient and the eavesdropper's channel coefficient are randomly generated using an i.i.d. complex Gaussian distribution with zero mean and unit variance. The temporal correlation parameters of the two channel coefficients are assumed to follow the Clarke's model and are characterized by $\rho_b = J_0(2\pi f_b \tau_d)$ and $\rho_e = J_0(2\pi f_e \tau_d)$, respectively. All the results to be shown are averaged over 10,000 channel trials. It is evident from Figs. 1, 2 and 3 that the Monte Carlo simulation points, marked by '$*$', match precisely with the analytical curves, which demonstrates the accuracy of our analysis.

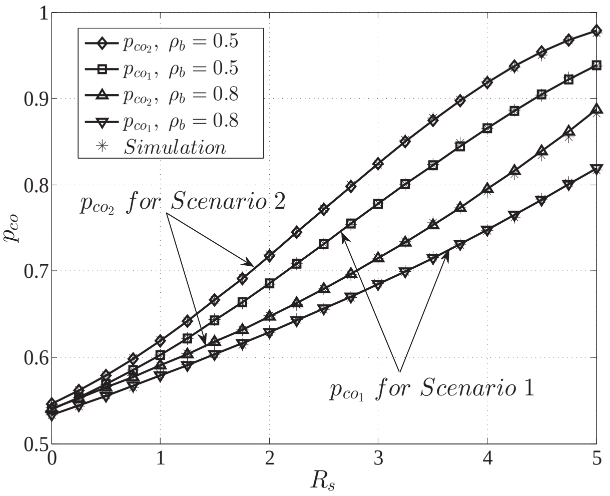

Fig. 1. Connection outage probability versus R_s with outdated CSI for $\bar{\gamma}_b = 10$ dB and $\bar{\gamma}_e = 0$ dB.

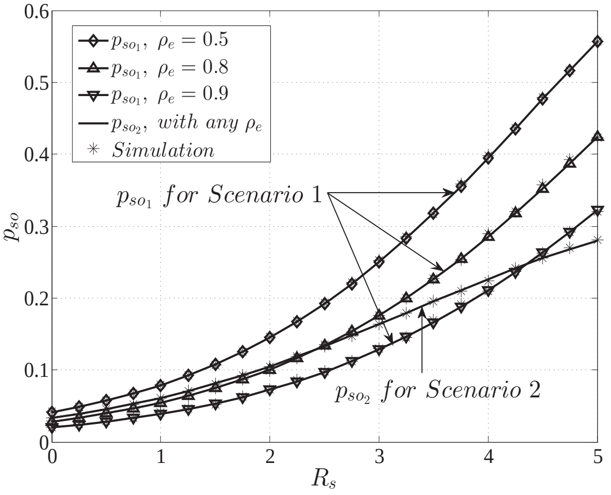

Fig. 2. Secrecy outage probability versus R_s with outdated CSI for $\bar{\gamma}_b = 10$ dB and $\bar{\gamma}_e = 0$ dB.

Fig. 1 plots the connection outage probability versus R_s for two scenarios with different values of ρ_b. In this figure, $p_{co_1}(R_s)$ and $p_{co_2}(R_s)$ are generated from (12) and (29), respectively. We first observe that $p_{co_1}(R_s)$ and $p_{co_2}(R_s)$ increase with R_s. This is due to the fact that an increasing R_s requires a higher C_b to satisfy the transmission condition. Notably, a higher C_b leads to a higher probability that $\tilde{C}_b$ is lower than C_b, due to the characteristics of Gauss-Markov process. Second, we observe that $p_{co_1}(R_s)$ and $p_{co_2}(R_s)$ increase when ρ_b decreases. This observation is not surprising since the uncertainty in the main channel quality increases as ρ_b decreases, which results in a poorer reliability. Third, we observe that $p_{co_2}(R_s)$ is higher than $p_{co_1}(R_s)$ for the same ρ_b. This is due to the fact that the transmission condition in *Scenario 2*, $C_b \geq \bar{C}_e + R_s$, is stricter than that in *Scenario 1*, $C_b \geq C_e + R_s$. Thus, a higher C_b is required in *Scenario 2*, which results in the worse reliability. Fourth, we observe that both $p_{co_1}(R_s)$ and $p_{co_2}(R_s)$ are always greater than 0.5, which implies that the reliability constraint should be loose in the on-off transmission schemes.

Fig. 2 plots the secrecy outage probability versus R_s for two scenarios with different values of ρ_e. In this figure, $p_{so_1}(R_s)$ and $p_{so_2}(R_s)$ are generated from (14) and (31), respectively.

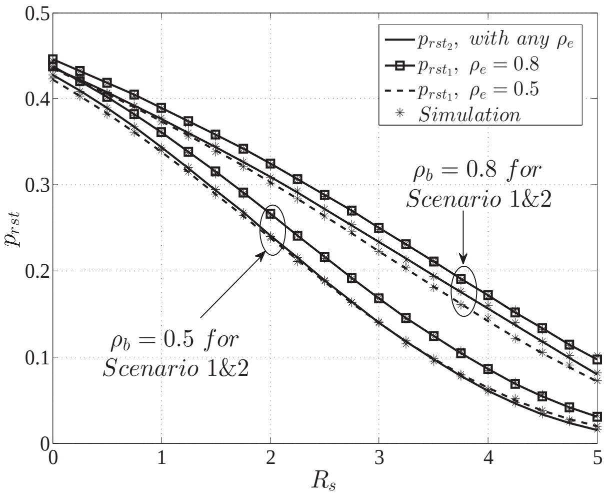

Fig. 3. Reliable and secure transmission probability versus R_s with outdated CSI for $\overline{\gamma}_b = 10$ dB and $\overline{\gamma}_e = 0$ dB.

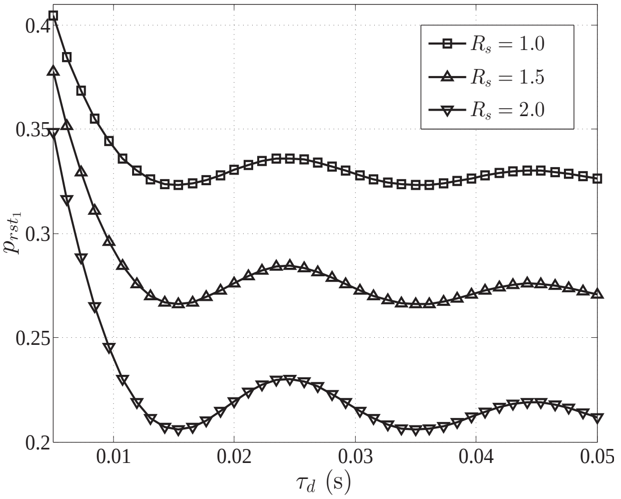

Fig. 4. Reliable and secure transmission probability versus τ_d for $\overline{\gamma}_b = 10$ dB, $\overline{\gamma}_e = 0$ dB, $v_b = v_e = 30$ km/h and $f_c = 900$ MHz in *Scenario 1*.

First, we observe that $p_{so_1}(R_s)$ and $p_{so_2}(R_s)$ increase as R_s increases. This is due to the fact that the rate redundancy, $C_b - R_s$, decreases with R_s and a lower rate redundancy leads to a higher probability that $\tilde{C}_e$ is higher than the rate redundancy. We then find that $p_{so_2}(R_s)$ is not influenced by the value of ρ_e and different behavior of $p_{so_1}(R_s)$ is observed depending on the value of ρ_e, as indicated by (31). When ρ_e is not sufficiently high (e.g. $\rho_e \leq 0.5$), $p_{so_1}(R_s)$ is always higher than $p_{so_2}(R_s)$; however, when ρ_e is sufficiently high (e.g. $\rho_e > 0.9$), the opposite happens. From a design perspective, this observation implies that C_e should be used for transmission design only when ρ_e is high; otherwise directly using $\bar{C}_e$ is a better choice for security enhancement. Moreover, we find that $p_{so_1}(R_s)$ and $p_{so_2}(R_s)$ are smaller than 0.1 for low R_s, which implies that the security constraint can be sufficiently strict in the on-off transmission schemes.

Fig. 3 plots the reliable and secrecy transmission probability versus R_s for two scenarios with different values of ρ_b and ρ_e. In this figure, $p_{rst_1}(R_s)$ and $p_{rst_2}(R_s)$ are generated from (18) and (33), respectively. We first observe that $p_{rst_1}(R_s)$ and $p_{rst_2}(R_s)$ decrease as R_s increases. This is due to the fact that increasing R_s strengthens the transmission condition (requiring higher C_b), which leads to a lower probability that $\tilde{C}_b$ is higher than C_b while the rate redundancy is higher than $\tilde{C}_e$. We also observe that $p_{rst_1}(R_s)$ and $p_{rst_2}(R_s)$ decrease when ρ_b decreases. Moreover, for a fixed ρ_b in *Scenario 1*, $p_{rst_1}(R_s)$ also decreases when ρ_e decreases. This is because that the uncertainty in the main and eavesdropper's channel quality increases as ρ_b and ρ_e decrease, which results in poorer reliability and security levels. Furthermore, we observe that for a fixed ρ_b, when ρ_e is high (e.g. $\rho_e = 0.8$), $p_{rst_1}(R_s)$ is higher than $p_{rst_2}(R_s)$; but when ρ_e is low (e.g. $\rho_e = 0.5$), $p_{rst_1}(R_s)$ is lower than $p_{rst_2}(R_s)$. This observation demonstrates that in terms of the reliable and secrecy transmission probability, a sufficiently high ρ_e is required to guarantee that *Scenario 1* performs better than *Scenario 2*.

Fig. 4 plots the reliable and secure transmission probability versus τ_d for *Scenario 1* with different values of R_s. The correlation coefficients are generated by the Clark's fading model with $v_b = v_e = 30$ km/h and $f_c = 900$ MHz. We first observe that $p_{rst_1}(R_s)$ is not a monotony decrease function of τ_d. In particular, we find that $p_{rst_1}(R_s)$ decreases fast before τ_d increases to 10 ms. However, when τ_d is sufficiently large, i.e., $\tau_d > 10$ ms, $p_{rst_1}(R_s)$ starts to fluctuate around a certain value and does not decrease further. This observation is not surprising since the absolute values of ρ_b and ρ_e, generated by the Clark's fading model, fluctuate in the large delay regime. Moreover, we observe that for a fixed τ_d, $p_{rst_1}(R_s)$ decreases as R_s increases, which has been explained in the descriptions of Fig. 3. Similarly, we conclude that $p_{rst_2}(R_s)$ versus τ_d for *Scenario 2* has a similar conclusion. The detailed illustrations for *Scenario 2* are omitted in this subsection to avoid redundancy.

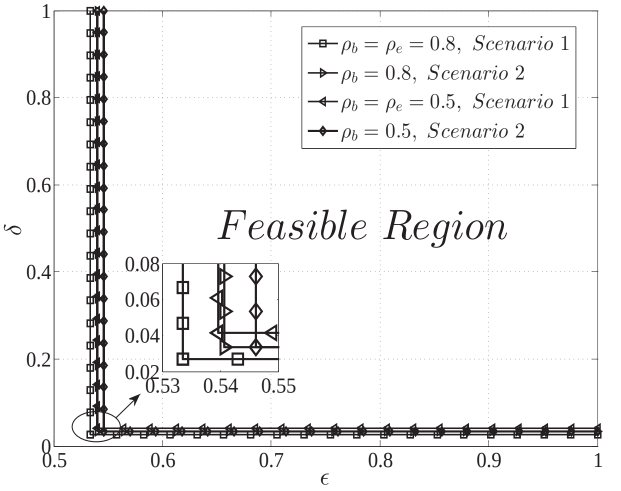

Fig. 5. Feasible security constraint versus feasible reliability constraint with outdated CSI for $\overline{\gamma}_b = 10$ dB and $\overline{\gamma}_e = 0$ dB.

Fig. 5 plots the feasible security constraint versus the feasible reliability constraint for both scenarios. In this figure, $p_{co_1,LB}$, $p_{so_1,LB}$, $p_{co_2,LB}$, and $p_{so_2,LB}$ are generated from (23), (25), (36), and (38), respectively. For each scenario with specifical ρ_b and ρ_e (only ρ_e in *Scenario 2*), the feasible region of ϵ and δ lies in the region above the corresponding curve. First, we observe that in both *Scenario 1* and *Scenario 2* increasing ρ_b leads to the extension of the feasible region. Second, we observe that the feasible region in *Scenario 2* is not influenced by ρ_e; while in *Scenario 1* we observe the extension in the feasible region when ρ_e increases. Third, we observe that for the same ρ_b, *Scenario 1* enables higher reliability level than *Scenario 2*. However, in terms of the security level, whether *Scenario 1* performs better or not depends on the value of ρ_e. In particular, *Scenario 1* enables higher security level when ρ_e is high (e.g. $\rho_e = 0.8$); while *Scenario 2* enables higher security level when ρ_e is low(e.g. $\rho_e = 0.5$). Fourth, we observe that the feasible regions are strictly restricted at the right side of $\epsilon = 0.5$, which implies that this transmission design ignores the system reliability and can be only applied for the systems where the reliability is not seen as important.

IV. Secure Transmission Design

In this section, we first investigate the optimal solutions for R_s meeting (9) for each scenario, based on which we then present numerical results to investigate the impact of the dual outage constraints on the secrecy throughput in both scenarios.

A. Optimized R_s for Scenario 1

In *Scenario 1*, the secrecy throughput is given by

$$\eta_1 (R_s) = p_{tx_1} (R_s) p_{rst_1} (R_s) R_s. \tag{40}$$

Mathematically, we express S_1 as

$$S_1 = \underset{R_s}{\operatorname{argmax}} \quad \eta_1 (R_s). \tag{41}$$

Using the mathematical software package to take the first-order derivative of $\eta_1 (R_s)$ with respect to R_s, we find that $\partial\eta_1 (R_s)/\partial R_s$ is first positive and then negative, which confirms that without dual outage constraints there is a unique solution to S_1, which achieves the maximum $\eta_1 (R_s)$.

Based on the feasibility for the dual outage constraints presented in (24) and (26), we express S_2 and S_3 as

$$S_2 = \{R_s \,|p_{co_1} (R_s) = \epsilon\}, \tag{42}$$

and

$$S_3 = \{R_s \,|p_{so_1} (R_s) = \delta\}, \tag{43}$$

respectively. As mentioned in Section III-A, both $p_{co_1} (R_s)$ and $p_{so_1} (R_s)$ are monotonous increasing functions of R_s, which guarantees that both (42) and (43) each have a unique solution.

Although the closed-form solutions for S_1, S_2, and S_3 are mathematically intractable, we are able to obtain them using a numerical method, e.g., bisection method. Based on above results, we present the optimal R_s that meets (9) in *Scenario 1* in the following proposition.

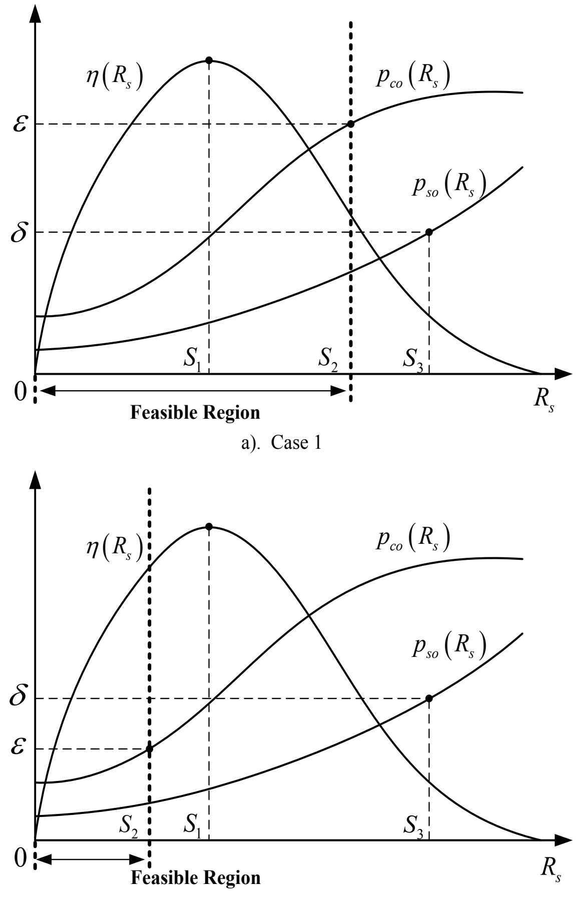

a). Case 1

b). Case 2

Fig. 6. Tho optimal R_s maximizing the secrecy throughput with dual outage constraints.

Proposition 1: The optimal R_s that maximizes the secrecy throughput *in Scenario 1*, subject to the connection and secrecy constraints, is given by

$$R^*_{s_1} = \min\{S_1, S_2, S_3\}, \tag{44}$$

where S_1, S_2, and S_3 are given by (41), (42), and (43), respectively.

Proof: By solving (41), (42), and (43), the values of S_1, S_2, and S_3 can be obtained, as depicted in Fig. 6. For a given ϵ and δ, the optimized R_s must lie within not only the feasible region determined by S_2 but the feasible region determined by S_3. As such, the feasible region of R_s is $\mathbb{S} = [0, \min\{S_2, S_3\}]$. Based on $\mathbb{S}$, we obtain the optimal R_s maximizing the secrecy throughput with dual outage constraints in the following two cases:

- If $S_1 < \min\{S_2, S_3\}$, as depicted in Fig. 6a), S_1 lies within the feasible region $\mathbb{S}$. That is, the maximum $\eta_1 (R_s)$ is still available in the feasible region $\mathbb{S}$, and S_1 is the unique solution. Hence, we have $R^*_{s_1} = S_1$. We highlight that in this case the outage constraints impose no effects on the optimal solution.
- If $S_1 \geq \min\{S_2, S_3\}$, as depicted in Fig. 6b), S_1 lies beyond the feasible region $\mathbb{S}$ and cannot be treated as the solution. Moreover, we find that $\eta_1 (R_s)$ is a monotonous

increasing function of R_s in the feasible region $\mathbb{S}$. As such, we take $R^*_{s_1} = \min\{S_2, S_3\}$ to guarantee that the highest secrecy throughput can be obtained.

To sum up the conclusions in the aforementioned two cases, the optimal R_s maximizing the secrecy throughput with dual outage constraints in (44) can be obtained. ■

B. Optimized R_s for Scenario 2

In *Scenario 2*, the secrecy throughput is given by

$$\eta_2(R_s) = p_{tx_2}(R_s)\, p_{rst_2}(R_s)\, R_s. \tag{45}$$

Mathematically, we express T_1 as

$$T_1 = \underset{R_s}{\operatorname{argmax}} \quad \eta_2(R_s). \tag{46}$$

We first use the mathematical software package to take the first-order derivative of $\eta_2(R_s)$ with respect to R_s and find that $\partial\eta_2(R_s)/\partial R_s$ is first positive and then negative. This indicates that there is a unique value of R_s maximizing $\eta_2(R_s)$ subject to no outage constraints. Hence we conclude that (46) has a unique solution.

Based on the feasibility for the dual outage constraints presented in (37) and (39), we express T_2 and T_3 as

$$T_2 = \{R_s \,|p_{co_2}(R_s) = \epsilon\}, \tag{47}$$

and

$$\begin{aligned} T_3 &= \{R_s \,|p_{so_2}(R_s) = \delta\} \\ &= \begin{cases} \log_2\left(\frac{\delta\overline{\gamma}_b}{[\exp(-1)-\delta]\overline{\gamma}_e}\right), & \delta < \exp(-1) \\ \infty, & \delta \geq \exp(-1), \end{cases} \end{aligned} \tag{48}$$

respectively. As mentioned in Section III-B, $p_{co_2}(R_s)$ is a monotonous increasing function of R_s, which implies that (47) has a unique solution.

Despite that the closed-form solutions for T_1 and T_2 are mathematically intractable, we are still able to obtain them using a numerical method, e.g., bisection method. Based on above results, we present the optimal R_s that meets (9) in *Scenario 2* in the following proposition.

Proposition 2: The optimal R_s that maximizes the secrecy throughput *in Scenario 2*, subject to two constraints, is given by

$$R^*_{s_2} = \min\{T_1, T_2, T_3\}, \tag{49}$$

where T_1, T_2, and T_3 are given by (46), (47), and (48) respectively.

Proof: The proof is similar with the proof for ***Proposition 1***. Here we omit the detailed proving process for brevity. ■

C. Numerical Results

In this subsection, we present numerical results to investigate the impact of the dual outage constraints on the secrecy throughput in each scenario. Since our analytical results have been verified using Monte Carlo simulations in Section III-C, the Monte Carlo simulation points are omitted in this subsection to avoid unnecessarily cluttering.

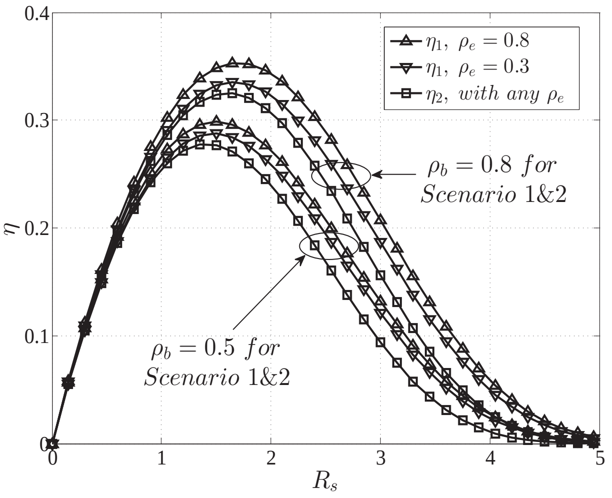

Fig. 7. Secrecy throughput subject to no outage constraints with outdated CSI for $\overline{\gamma}_b = 10$ dB and $\overline{\gamma}_e = 0$ dB.

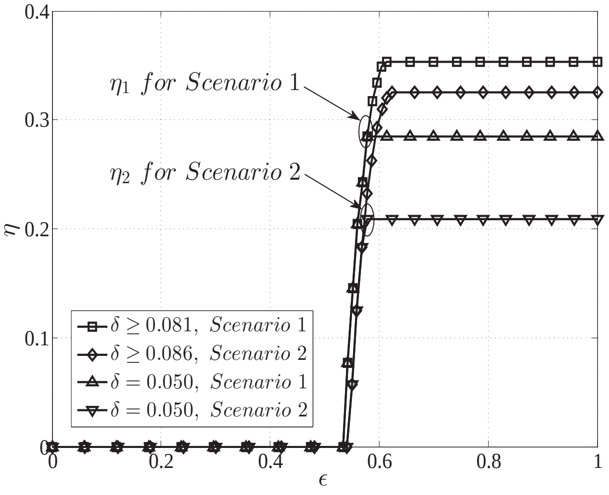

Fig. 8. Secrecy throughput versus reliability constraint with outdated CSI for $\rho_b = \rho_e = 0.8$, $\overline{\gamma}_b = 10$ dB and $\overline{\gamma}_e = 0$ dB.

Fig. 7 plots the secrecy throughput versus R_s for two scenarios with different values of ρ_b and ρ_e. In this figure, we generate $\eta_1(R_s)$ and $\eta_2(R_s)$ from (40) and (45), respectively. Moreover, we do not consider the reliability and security constraints such that $\epsilon = \delta = 1$. Moreover, we do not consider the reliability and security constraints such that $\epsilon = \delta = 1$. We first observe that the secrecy throughput first increases and then decreases as R_s increases, indicating that an optimal R_s indeed exists such that the secrecy throughput is maximized. Thus we clarify that (41) and (46) each have a unique solution. We also observe that the secrecy throughput decreases when ρ_b or ρ_e decreases. Furthermore, we observe that for the same ρ_b, the secrecy throughput in *Scenario 1* is higher than that in *Scenario 2*, even if ρ_e is fairly low (e.g. $\rho_e = 0.3$). This is due to the fact that there is a higher probability to perform transmission in *Scenario 1* than that in *Scenario 2*. Thus *Scenario 1* offers a better secrecy throughput than *Scenario 2* without the outage constraints.

Fig. 8 and Fig. 9 plot the secrecy throughput for two

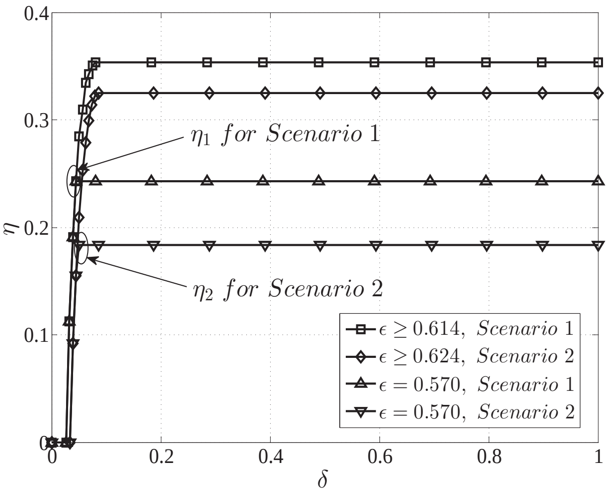

Fig. 9. Secrecy throughput versus security constraint with outdated CSI for $\rho_b = \rho_e = 0.8$, $\overline{\gamma}_b = 10$ dB and $\overline{\gamma}_e = 0$dB.

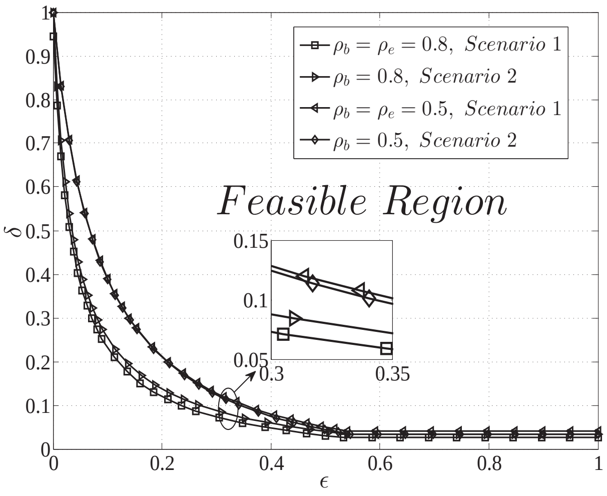

Fig. 10. Feasible security constraint versus feasible reliability constraint with outdated CSI for $\overline{\gamma}_b = 10$ dB and $\overline{\gamma}_e = 0$ dB.

scenarios versus the reliability constraint and the security constraint, respectively. We first observe that the secrecy throughput is a monotone non-decreasing function of either constraint. We then see that a positive secrecy throughput is achieved only when the two constraints are within the feasible ranges. For example, in Fig. 8 a positive secrecy throughput is achieved when $0.534 < \epsilon \leq 1$ in *Scenario 1* and when $0.541 < \epsilon \leq 1$ in *Scenario 2*. Moreover, in Fig. 9 a positive secrecy throughput is achieved when $0.027 < \delta \leq 1$ in *Scenario 1* and when $0.034 < \delta \leq 1$ in *Scenario 2*. Notably, we find that in the specifical case with $\rho_b = \rho_e = 0.8$, *Scenario 1* has a stricter security constraint and a stricter reliability constraint than *Scenario 2*. Furthermore, we observe that a constraint threshold exists such that the secrecy throughput keeps constant after the constraint exceeds the threshold. For example, it is seen from Fig. 8 and 9 that the maximum secrecy throughput in *Scenario 1* is achieved when $\epsilon \geq 0.614$ and $\delta \geq 0.081$, and the maximum secrecy throughput in *Scenario 2* is achieved when $\epsilon \geq 0.624$ and $\delta \geq 0.086$. This is due to the fact that the optimal R_s can always be used to perform data transmission with the same secrecy throughput when the constraints are higher than the thresholds.

V. Discussions

As seen in Section IV, R_s is the only controllable parameter for transmission design. Our solutions of the optimal R_s allow us to maximize the secrecy throughput subject to two constraints. We also note that the designed transmission schemes forgo the reliability level, as seen in Fig. 5. This is due to the fact that in the presence of the outdated CSI, the main channel quality known at Alice tends to be higher than the instantaneous channel capacity for secure transmission. As such, this transmission design may not be suitable for the systems where the reliability is in high demand. Motivated by this, in this section we present some discussions about the possible transmission design to improve reliability level.

Based on the aforementioned reasons, we believe that the use of $R_b = C_b$ makes the quality of the main channel to be overestimated. Thus it is wise for Alice to set R_b as

$$R_b = \log_2\left(2^{R_s} + u\left(2^{C_b} - 2^{R_s}\right)\right), \tag{50}$$

where $u \in [0, 1]$. Note that when $u = 1$ we have $R_b = C_b$, and when $u = 0$ we have $R_b = R_s$. It is evident from (50) that the value of R_b is within the feasible range of $[R_s, C_b]$.

By applying (50) into the system model in Section II-B and using the similar approaches in Section III, we can derive the closed-form expressions of $p_{co_1}(u, R_s)$, $p_{so_1}(u, R_s)$, $p_{co_2}(u, R_s)$ and $p_{so_2}(u, R_s)$. Thus the lower bounds on these outage probabilities for a given u, such as $p_{co_1,LB}(u)$, $p_{so_1,LB}(u)$, $p_{co_2,LB}(u)$ and $p_{so_2,LB}(u)$, can be obtained by setting $R_s = 0$. Here the detailed derivations are omitted for brevity. We then find that the choice of R_b, indicated by (50), enables a trade-off between the feasible reliability constraint and the feasible security constraint. For example, a lower R_b leads to a lower connection outage probability but a higher secrecy outage probability. This implies that if we set a looser reliability constraint, the security constraint becomes stricter.

To illustrate this trade-off between the feasible reliability constraint and the feasible security constraint, Fig. 10 plots the new feasible region of the dual outage constraints for both scenarios. In this figure, the curves are generated by using the values of $p_{co_1,LB}(u)$, $p_{so_1,LB}(u)$, $p_{co_2,LB}(u)$ and $p_{so_2,LB}(u)$ at all values of u. For each scenario with fixed ρ_b and ρ_e, the feasible region of ϵ and δ lies in the region above the corresponding curve. We first observe that when u increases, the lower bound on the connection outage probability increases, but the lower bound on the secrecy outage probability decreases. For example, in *Scenario 2* when u increases from 0 to 1, the lower bound on the connection outage probability increases from 0 to $p_{co_2,LB}$, as indicated by (36), while the lower bound on the secrecy outage probability decreases from 1 to $p_{so_2,LB}$, as indicated by (38). This observation is not surprising since allowing more freedom on R_b enables a trade-off between reliability and security. Notably, this trade-off leads to a profound extension in the feasible region compared with Fig. 5. We also observe the extension of the feasible region when ρ_b or ρ_e increases, which is due to that the uncertainty in the main channel and the eavesdropper's channel decreases when ρ_b and ρ_e increase, respectively. This indicates that the more knowledge about the channel quality is known at Alice, the better reliability and security levels can be achieved.

VI. Conclusion

In the presence of outdated CSI, we adopted the on-off scheme to help perform secure transmission, under which we conducted the secrecy performance in wiretap channel and then presented the design of wiretap coding parameters. In particular, we considered the two scenarios with different assumptions on the CSI from the eavesdropper. For each scenario, we derived the transmission probability, the connection outage probability, the secrecy outage probability as well as the reliable and secure transmission probability. Based on these results, we determined the optimal secrecy rates that maximize the secrecy throughput under dual connection and secrecy outage constraints. Moreover, we found that a larger feasible region of the dual outage constraints can be obtained by optimizing the codeword transmission rate.

Appendix A
Derivation of $p_{co_1}(R_s)$ in (12)

Based on (11), we formulate $p_{co_1}(R_s)$ as

$$\begin{aligned} p_{co_1}(R_s) &= \Pr\left\{\tilde{C}_b < C_b \left| C_b - C_e \ge R_s \right.\right\} \\ &= \Pr\left\{\tilde{\gamma}_b < \gamma_b \left| \gamma_b \ge 2^{R_s}(1+\gamma_e) - 1 \right.\right\} \\ &= \frac{\Pr\left\{\tilde{\gamma}_b < \gamma_b, \gamma_b \ge 2^{R_s}(1+\gamma_e) - 1\right\}}{\Pr\left\{\gamma_b \ge 2^{R_s}(1+\gamma_e) - 1\right\}}. \end{aligned} \tag{51}$$

We first re-express the numerator of $p_{co_1}(R_s)$ as

$$\begin{aligned} &\Pr\left\{\tilde{\gamma}_b < \gamma_b, \gamma_b \ge 2^{R_s}(1+\gamma_e) - 1\right\} \\ =& \int_0^\infty \underbrace{\int_{2^{R_s}(1+x)-1}^\infty \underbrace{\int_0^y f_{\tilde{\gamma}_b|\gamma_b}(z|y)\,dz}_{\Xi_1} f_{\gamma_b}(y)\,dy}_{\Xi_2} f_{\gamma_e}(x)\,dx. \end{aligned} \tag{52}$$

Recall that $\tilde{\gamma}_b$ and γ_b are two correlated exponential random variables (RVs). The conditional PDF of $\tilde{\gamma}_b$ conditioned on a given γ_b is given by

$$\begin{aligned} f_{\tilde{\gamma}_b|\gamma_b}(z|y) =& \frac{1}{(1-\rho_b^2)\bar{\gamma}_b} \exp\left(-\frac{z+\rho_b^2 y}{(1-\rho_b^2)\bar{\gamma}_b}\right) \\ &\times I_0\left(\frac{2\rho_b\sqrt{zy}}{(1-\rho_b^2)\bar{\gamma}_b}\right). \end{aligned} \tag{53}$$

Substituting (53) into Ξ_1, we derive Ξ_1 as

$$\Xi_1 = 1 - Q_1\left(\sqrt{\frac{2\rho_b^2 y}{(1-\rho_b^2)\bar{\gamma}_b}}, \sqrt{\frac{2y}{(1-\rho_b^2)\bar{\gamma}_b}}\right), \tag{54}$$

where $Q_1(a,b)$ represents the Marcum's Q-function [34]. We then use the series representation of Marcum's Q-function in terms of Bessel functions, given by

$$Q_1(a,b) = \exp\left(-\frac{a^2+b^2}{2}\right)\sum_{n=0}^\infty \left(\frac{a}{b}\right)^n I_n(ab), \tag{55}$$

and the expansion of Bessel function [33, Eq. (8.445)], given by

$$I_v(z) = \sum_{k=0}^\infty \frac{1}{k!\Gamma(v+k+1)}\left(\frac{z}{2}\right)^{v+2k}, \tag{56}$$

to obtain the series representation of Ξ_1, which yields

$$\begin{aligned} \Xi_1 =& 1 - \exp\left(-\frac{(1+\rho_b^2)y}{(1-\rho_b^2)\bar{\gamma}_b}\right)\sum_{n=0}^\infty\sum_{k=0}^\infty \frac{\rho_b^{2(n+k)}}{k!} \\ &\times \frac{1}{\Gamma(n+k+1)}\left(\frac{y}{(1-\rho_b^2)\bar{\gamma}_b}\right)^{n+2k}. \end{aligned} \tag{57}$$

Substituting (57) into Ξ_2, we derive Ξ_2 as

$$\begin{aligned} \Xi_2 =& \exp\left(-\frac{2^{R_s}x + 2^{R_s} - 1}{\bar{\gamma}_b}\right) - \exp\left(-\frac{2\left(2^{R_s}-1\right)}{(1-\rho_b^2)\bar{\gamma}_b}\right) \\ &\times \exp\left(-\frac{2^{1+R_s}x}{(1-\rho_b^2)\bar{\gamma}_b}\right)\sum_{n=0}^\infty\sum_{k=0}^\infty \frac{\rho_b^{2(n+k)}\left(1-\rho_b^2\right)}{k!2^{n+2k+1}} \\ &\times \frac{(n+2k)!}{(n+k)!}\sum_{m=0}^{n+2k}\sum_{q=0}^{m} \frac{\left(2^{R_s}-1\right)^{m-q}2^{m+qR_s}x^q}{q!(m-q)!((1-\rho_b^2)\bar{\gamma}_b)^m}. \end{aligned} \tag{58}$$

Substituting (58) into (52) and solve the resultant integrals, the numerator of $p_{co_1}(R_s)$ is obtained. We also note that the denominator of $p_{co_1}(R_s)$ is given by (10). Therefore, we obtain $p_{co_1}(R_s)$ in (12).

Appendix B
Derivation of $p_{so_1}(R_s)$ in (14)

Based on (13), we formulate $p_{so_1}(R_s)$ as

$$\begin{aligned} &p_{so_1}(R_s) = \Pr\left\{C_b - R_s < \tilde{C}_e \left| C_b - C_e \ge R_s \right.\right\} \\ &= \Pr\left\{\gamma_b < 2^{R_s}(1+\tilde{\gamma}_e) - 1 \left| \gamma_b \ge 2^{R_s}(1+\gamma_e) - 1 \right.\right\} \\ &= \frac{\Pr\left\{\gamma_b < 2^{R_s}(1+\tilde{\gamma}_e) - 1, \gamma_b \ge 2^{R_s}(1+\gamma_e) - 1\right\}}{\Pr\left\{\gamma_b \ge 2^{R_s}(1+\gamma_e) - 1\right\}}. \end{aligned} \tag{59}$$

We re-express the numerator of $p_{so_1}(R_s)$ as

$$\begin{aligned} &\Pr\left\{\gamma_b < 2^{R_s}(1+\tilde{\gamma}_e) - 1, \gamma_b \ge 2^{R_s}(1+\gamma_e) - 1\right\} \\ &= \Pr\left\{\tilde{\gamma}_e > 2^{-R_s}(1+\gamma_b) - 1, \gamma_e \le 2^{-R_s}(1+\gamma_b) - 1\right\} \\ &= \int_{2^{R_s}-1}^\infty \underbrace{\int_0^{2^{-R_s}(1+x)-1} \Phi_1 f_{\gamma_e}(y)\,dy}_{\Phi_2} f_{\gamma_b}(x)\,dx, \end{aligned} \tag{60}$$

where Φ_1 is

$$\Phi_1 = \int_{2^{-R_s}(1+x)-1}^\infty f_{\tilde{\gamma}_e|\gamma_e}(z|y)\,dz. \tag{61}$$

Recall that $\tilde{\gamma}_e$ and γ_e are two correlated exponential RVs. The conditional PDF of $\tilde{\gamma}_e$ conditioned on a given γ_e is given by

$$\begin{aligned} f_{\tilde{\gamma}_e|\gamma_e}\left(z\left|y\right.\right) = & \frac{1}{\left(1-\rho_e^2\right)\bar{\gamma}_e}\exp\left(-\frac{z+\rho_e^2 y}{\left(1-\rho_e^2\right)\bar{\gamma}_e}\right) \\ & \times I_0\left(\frac{2\rho_e\sqrt{zy}}{\left(1-\rho_e^2\right)\bar{\gamma}_e}\right). \end{aligned} \tag{62}$$

We then substitute (62) into (61) to derive Φ_1 as

$$\Phi_1 = Q_1\left(\sqrt{\frac{2\rho_e^2 y}{\left(1-\rho_e^2\right)\bar{\gamma}_e}},\sqrt{\frac{2^{1-R_s}\left(x+1\right)-2}{\left(1-\rho_e^2\right)\bar{\gamma}_e}}\right). \tag{63}$$

With the help of (55) and (56), the series representation of Φ_1 is obtained as

$$\begin{aligned} \Phi_1 = & \exp\left(-\frac{\rho_e^2 y + 2^{-R_s}x + 2^{-R_s}-1}{\left(1-\rho_e^2\right)\bar{\gamma}_e}\right)\sum_{n=0}^{\infty}\sum_{k=0}^{\infty}\frac{1}{k!} \\ & \times\frac{\rho_e^{2(n+k)}y^{n+k}\left(2^{-R_s}x+2^{-R_s}-1\right)^k}{\Gamma\left(n+k+1\right)\left(\left(1-\rho_e^2\right)\bar{\gamma}_e\right)^{n+2k}}. \end{aligned} \tag{64}$$

Substituting (64) into Φ_2, we obtain the series representation of Φ_2 as

$$\begin{aligned} \Phi_2 = & \exp\left(-\frac{x+1-2^{R_s}}{\left(1-\rho_e^2\right)2^{R_s}\bar{\gamma}_e}\right)\sum_{n=0}^{\infty}\sum_{k=0}^{\infty}\frac{\rho_e^{2(n+k)}\left(1-\rho_e^2\right)}{k!(\left(1-\rho_e^2\right)\bar{\gamma}_e)^k} \\ & \times\left(\frac{x+1-2^{R_s}}{2^{R_s}}\right)^k\left[1-\exp\left(-\frac{x+1-2^{R_s}}{\left(1-\rho_e^2\right)2^{R_s}\bar{\gamma}_e}\right)\right. \\ & \left.\times\sum_{m=0}^{n+k}\frac{1}{m!}\left(\frac{x+1-2^{R_s}}{\left(1-\rho_e^2\right)2^{R_s}\bar{\gamma}_e}\right)^m\right]. \end{aligned} \tag{65}$$

Finally, we substitute (65) into (60) and solve the resultant integrals to obtain numerator of $p_{so_1}\left(R_s\right)$. Hence, $p_{so_1}\left(R_s\right)$ in (14) can be obtained.

Appendix C
Derivation of $p_{rst_1}\left(R_s\right)$ in (18)

Based on (17), we formulate $p_{rst_1}\left(R_s\right)$ as

$$\begin{aligned} p_{rst_1}\left(R_s\right) & = \Pr\left\{\tilde{C}_b \geq C_b, C_b - R_s \geq \tilde{C}_e\left|C_b - C_e \geq R_s\right.\right\} \\ & = \Pr\left\{\tilde{\gamma}_b \geq \gamma_b, \gamma_b \geq 2^{R_s}\left(1+\tilde{\gamma}_e\right)-1\left|\gamma_b \geq 2^{R_s}\left(1+\gamma_e\right)-1\right.\right\} \\ & = \frac{\Pr\left\{\tilde{\gamma}_b \geq \gamma_b, \gamma_b \geq 2^{R_s}\left(1+\tilde{\gamma}_e\right)-1, \gamma_b \geq 2^{R_s}\left(1+\gamma_e\right)-1\right\}}{\Pr\left\{\gamma_b \geq 2^{R_s}\left(1+\gamma_e\right)-1\right\}}. \end{aligned} \tag{66}$$

By re-expressing the numerator of $p_{rst_1}\left(R_s\right)$ we obtain

$$\begin{aligned} & \Pr\left\{\tilde{\gamma}_b \geq \gamma_b, \tilde{\gamma}_e \leq \frac{1+\gamma_b}{2^{R_s}}-1, \gamma_e \leq \frac{1+\gamma_b}{2^{R_s}}-1\right\} \\ & = \int_{2^{R_s}-1}^{\infty}\Delta_1\Delta_2 f_{\gamma_b}\left(x\right)dx, \end{aligned} \tag{67}$$

where Δ_1 is

$$\Delta_1 = \Pr\left\{\tilde{\gamma}_b \geq x\right\} = \int_x^{\infty} f_{\tilde{\gamma}_b|\gamma_b}\left(w\left|x\right.\right)dw, \tag{68}$$

and Δ_2 is

$$\begin{aligned} \Delta_2 & = \Pr\left\{\tilde{\gamma}_e \leq 2^{-R_s}\left(1+x\right)-1, \gamma_e \leq 2^{-R_s}\left(1+x\right)-1\right\} \\ & = \int_0^{2^{-R_s}(1+x)-1}\int_0^{2^{-R_s}(1+x)-1} f_{\tilde{\gamma}_e|\gamma_e}\left(z\left|y\right.\right)dz f_{\gamma_e}\left(y\right)dy. \end{aligned} \tag{69}$$

With the help of Ξ_1 in Appendix A and Φ_2 in Appendix B, we obtain the series representations of Δ_1 and Δ_2 as

$$\Delta_1 = 1 - \Xi_1 \tag{70}$$

and

$$\Delta_2 = 1 - \exp\left(-\frac{2^{-R_s}x + 2^{-R_s}-1}{\bar{\gamma}_e}\right) - \Phi_2, \tag{71}$$

where Ξ_1 is given by (57) and Φ_2 is given by (65).

Finally, we substitute (70) and (71) into (67) and solve the resultant integrals, the numerator of $p_{rst_1}\left(R_s\right)$ is obtained. Using (10), $p_{rst_1}\left(R_s\right)$ in (18) can be obtained.

References

[1] H. V. Poor, "Information and inference in the wireless physical layer," *IEEE Wireless Commun.*, vol. 19, no. 1, pp. 40–47, Feb. 2012.

[2] B. Schneier, "Cryptographic design vulnerabilities," *Computer*, vol. 31, no. 9, pp. 29–33, Sep. 1998.

[3] X. Zhou, L. Song, and Y. Zhang, *Physical Layer Security in Wireless Communications.* CRC Pr., 2013.

[4] N. Yang, L. Wang, G. Geraci, M. Elkashlan, J. Yuan, and M. Di Renzo, "Safeguarding 5G wireless communication networks using physical layer security," *IEEE Commun. Mag.*, vol. 53, no. 4, pp. 20–27, Apr. 2015.

[5] C. E. Shannon, "Communication theory of secrecy systems," *Bell Syst. Techn. J.*, vol. 28, no. 4, pp. 656–715, Oct. 1949.

[6] A. D. Wyner, "The wire-tap channel," *Bell Syst. Techn. J.*, vol. 54, no. 8, pp. 1355–1387, Oct. 1975.

[7] I. Csiszàr and J. Körner, "Broadcast channels with confidential messages," *IEEE Trans. Inf. Theory*, vol. 24, no. 3, pp. 339–348, May 1978.

[8] S. K. Leung-Yan-Cheong and M. E. Hellman, "The Gaussian wiretap channel," *IEEE Trans. Inf. Theory*, vol. 24, no. 4, pp. 451–456, July 1978.

[9] H. Alves, R. D. Souza, M. Debbah, and M. Bennis, "Performance of transmit antenna selection physical layer security schemes," *IEEE Signal Process. Lett.*, vol. 19, no. 6, pp. 372–375, June 2012.

[10] N. Yang, P. L. Yeoh, M. Elkashlan, R. Schober, and I. B. Collings, "Transmit antenna selection for security enhancement in MIMO wiretap channels," *IEEE Trans. Commun.*, vol. 61, no. 1, pp. 144–154, Jan. 2013.

[11] N. Yang, P. L. Yeoh, M. Elkashlan, R. Schober, and J. Yuan, "MIMO wiretap channels: Secure transmission using transmit antenna selection and receive generalized selection combining," *IEEE Commun. Lett.*, vol. 17, no. 9, pp. 1754–1757, Sep. 2013.

[12] N. Yang, H. A. Suraweera, I. B. Collings, and C. Yuen, "Physical layer security of TAS/MRC with antenna correlation," *IEEE Trans. Inf. Forensics Security*, vol. 8, no. 1, pp. 254–259, Jan. 2013.

[13] J. Hu, Y. Cai, N. Yang, and W. Yang, "A new secure transmission scheme with outdated antenna selection," *IEEE Trans. Inf. Forensics Security*, accepted to appear.

[14] X. Zhou and M. R. McKay, "Secure transmission with artificial noise over fading channels: Achievable rate and optimal power allocation," *IEEE Trans. Veh. Technol.*, vol. 59, no. 8, pp. 3831–3842, Oct. 2010.

[15] A. Mukherjee and A. L. Swindlehurst, "Robust beamforming for security in MIMO wiretap channels with imperfect CSI," *IEEE Trans. Signal Process.*, vol. 59, no. 1, pp. 351–361, Jan. 2011.

[16] J. M. Taylor, M. Hempel, H. Sharif, S. Ma, and Y. Yang, "Impact of channel estimation errors on effectiveness of eigenvector-based jamming for physical layer security in wireless networks," in *Proc. IEEE CAMAD Workshop*, Kyoto, Japan, June 2011, pp. 122–126.

[17] T. Y. Liu, S. C. Lin, T. H. Chang, and Y. W. P. Hong, "How much training is enough for secrecy beamforming with artificial noise," in *Proc. IEEE Int. Conf. Commun.*, Ottawa, Canada, June 2012, pp. 4782–4787.

[18] M. Pei, J. Wei, K. K. Wong, and X. Wang, "Masked beamforming for multiuser MIMO wiretap channels with imperfect CSI," *IEEE Trans. Wireless Commun.*, vol. 11, no. 2, pp. 544–549, Feb. 2012.

[19] B. He, and X. Zhou, "Secrecy on-off transmission design with channel estimation errors," *IEEE Trans. Inf. Forensics Security*, vol. 8, no. 12, pp.1923–1936, Dec. 2013.

[20] S. Bashar, Z. Ding, and Y. Li, "On secrecy of codebook-based transmission beamforming under receiver limited feedback," *IEEE Trans. Wireless Commun.*, vol. 10, no. 4, pp. 1212–1223, Apr. 2011.

[21] S. C. Lin, T. H. Chang, Y. L. Liang, Y. W. P. Hong, and C. Y. Chi, "On the impact of quantized channel feedback in guaranteeing secrecy with artificial noise: The noise leakage problem," *IEEE Trans. Wireless Commun.*, vol. 10, no. 3, pp. 901–915, Mar. 2011.

[22] L. Sun and S. Jin, "On the ergodic secrecy rate of multiple-antenna wiretap channels using artificial noise and finite-rate feedback," in *Proc. IEEE Int. Symp. Personal Indoor Mobile Radio Commun.*, Toronto, Canada, Sep. 2011, pp. 1–5.

[23] Z. Rezki, A. Khisti, and M. S. Alouini, "On the ergodic secret message capacity of the wiretap channel with finite-rate feedback," in *Proc. IEEE Int. Symp. Inf. Theory*, Cambridge, America, Jul. 2012, pp. 239–243.

[24] X. Zhang, M. R. McKay, X. Zhou, and R. W. Heath Jr., "Artificial-noise-aided secure multi-antenna transmission with limited feedback," *IEEE Trans. Wireless Commun.*, vol. 14, no. 5, pp. 2742–2754, May 2015.

[25] Y. Yang, W. Wang, H. Zhao, and L. Zhao, "Transmitter beamforming and artificial noise with delayed feedback: Secrecy rate and power allocation," *J. Commun. Networks*, vol. 14, no. 4, pp. 374–384, Aug. 2012.

[26] N. S. Ferdinand, D. B. Costa, and M. Latva-aho, "Effects of outdated CSI on the secrecy performance of MISO wiretap channels with transmit antenna selection", *IEEE Commun. Lett.*, vol. 17, no. 5, pp. 864–867, May 2013.

[27] P. K. Gopala, L. Lai, and H. E. Gamal, "On the secrecy capacity of fading channels," *IEEE Trans. Inf. Theory*, vol. 54, no. 10, pp. 4687–4698, Oct. 2008.

[28] X. Zhou, M. R. McKay, B. Maham, and A. Hjørungnes, "Rethinking the secrecy outage formulation: A secure transmission design perspective," *IEEE Commun. Lett.*, vol. 15, no. 3, pp. 302–304, Mar. 2011.

[29] Y. Liang, H. V. Poor, and S. Shamai, "Secure communication over fading channels," *IEEE Trans. Inf. Theory*, vol. 54, no. 6, pp. 2470–2492, June 2008.

[30] A. Khisti and G. Wornell, "Secure transmission with multiple antennas – Part I: The MISOME wiretap channel," *IEEE Trans. Inf. Theory*, vol. 56, no. 7, pp. 3088–3104, July 2010.

[31] A. Khisti and G. Wornell, "Secure transmission with multiple antennas – Part II: The MIMOME wiretap channel," *IEEE Trans. Inf. Theory*, vol. 56, no. 11, pp. 5515–5532, Nov. 2010.

[32] D. S. Michalopoulos, H. A. Suraweera, G. K. Karagiannidis, and R. Schober, "Amplify-and-forward relay selection with outdated channel estimates", *IEEE Trans. Commun.*, vol. 60, no. 5, pp. 1278–1290, May 2012.

[33] I. S. Gradshteyn and I. M. Ryzhik, *Table of Integrals, Series and Products*, 7th Edition. Academic Press, 2007.

[34] J. I. Marcum, *Table of Q Functions*. Santa Monica, CA, USA: Rand Corporation, 1950.